Bimolecular Termination Events in the Seeded Emulsion Polymerization of Styrene

Mary E. Adams,† Gregory T. Russell, Brendan S. Casey, Robert G. Gilbert, and Donald H. Napper*

School of Chemistry, The University of Sydney, Sydney, NSW 2006, Australia

David F. Sangster

CSIRO Division of Chemicals and Polymers, Lucas Heights Research Laboratories, Private Bag 7, Menai, NSW 2234, Australia

Received October 17, 1989; Revised Manuscript Received March 15, 1990

ABSTRACT: Bimolecular termination processes in the seeded emulsion polymerization of styrene have been studied by using large seed particles and γ-ray initiation. The observed relaxation kinetics differed significantly from those previously found for methyl methacrylate in that the results could not be explained simply in terms of propagation-driven ("residual" or "reaction-diffusion") termination. The data have been successfully interpreted, however, by a "short-long" model that differentiates between free radicals attached to short chains, whose mobility is not significantly diminished by entanglements, and those attached to long, entangled chains. The latter are formed by the rapid growth to entanglement length of the former, whereas the short chains arise both from free-radical entry into the particles and from chain transfer to monomer by long chains. Bimolecular termination between short and long chains is the predominant radical-annihilation event. The dependence upon weight fraction of polymer of the rate coefficient obtained experimentally for short-long termination is in good agreement with that calculated from the rate of diffusion of short species through the latex particles. The relaxation-derived termination rate coefficients were also found to predict the experimentally observed Trommsdorff-Norrish gel effect in chemically initiated seeded emulsion polymerization systems.

Introduction

Bimolecular termination processes in free-radical polymerizations are intrinsically complex, whether or not such polymerizations are homogeneous or heterogeneous.[1-3] As the polymerizing system passes from zero to complete conversion, a number of domains may be traversed in which the nature of the rate-determining step for bimolecular termination varies quite dramatically. The reason for this is straightforward: the polymer that is formed in the reaction can exert a profound influence on subsequent termination events. What unifies the diverse range of termination processes spanning the entire range of conversions is that all are apparently diffusion controlled. They differ principally in the nature of the species that are involved in the rate-limiting processes.

Benson and North[4] considered that three consecutive diffusion steps were operative in bimolecular termination events. The first involves the center-of-mass (translational) diffusion of two macroradical species into close proximity. This then allows the second process, segmental diffusion, to bring the two free-radical chain ends sufficiently close together to allow the third step, chemical reaction, to ensue. The latter is so rapid that it is rarely, if ever, rate determining. At very low conversions in bulk systems, the segmental diffusion step is likely to be rate determining. As the weight fraction of dissolved polymer increases, however, the situation may be reached wherein chain entanglements so slow the center-of-mass diffusion that it becomes rate limiting.[2,3]

At even higher conversions, it might be expected that a third type of diffusion-controlled termination, so-called "residual termination", would manifest itself.[5-7] This occurs when chain entanglements so reduce the rate of translational diffusion of the macroradicals that the main contribution to the spatial mobility of the free-radical chain ends derives from the act of propagation. Such "reaction-diffusion" termination is residual in the sense that it is operative whenever monomer is present to allow propagation to occur. In this sense, it causes there to be an irreducible, minimum termination rate. Of course, the propagation step itself may also become diffusion controlled if, e.g., the polymer becomes glassy or the system is starved of monomer, as it may be in a continuous reactor. A theory that predicts the upper and lower bounds for the termination rate coefficient (k_t) when residual termination is operative has recently been proposed.[7]

Cardenas and O'Driscoll[8] have developed a theory for free-radical bulk polymerization at high conversions on the assumption that the population of radicals can be divided into two classes: those attached to chains of sufficient length to become entangled with preformed neighboring polymer molecules and thus exhibit restricted mobility; and those attached to shorter chains whose mobility is not substantially reduced by entanglements. Both Soh and Sundberg[9] and Olaj et al.[10] have considered theoretically some of the kinetic consequences of chain-length-dependent termination rate coefficients.

The foregoing theories, as well as those proposed to explain the Trommsdorff-Norrish, or gel, effect (see section on this phenomenon elsewhere in this paper), were developed primarily to describe bulk polymerizations. The extent to which these ideas can be applied to emulsion polymerizations is still an open question. In classical emulsion polymerizations, polymerization occurs primarily within the monomer-swollen latex particles so that some parallelism in behavior might be anticipated. The particles, however, usually contain a minimum weight fraction of polymer (w_p) of between one-third and a half so that the limiting zero-conversion value of the termination rate coefficient is rarely, if ever, applicable to emulsion

* Author to whom correspondence is addressed.
† Present address: Emulsion Polymers Institute, Mountaintop Campus, Lehigh University, Bethlehem, PA 18015.

0024-9297/90/2223-4624$02.50/0

polymerizations. Further, the onset of the Trommsdorff–Norrish autoacceleration in emulsion polymerizations often occurs at significantly higher weight fractions of polymer than in bulk polymerizations, perhaps implying a different origin for the decrease in termination rate coefficient from that in bulk.

It has previously been shown that the termination rate coefficients for methyl methacrylate in seeded emulsion polymerization systems could be measured by γ-radiation relaxation studies.[11] In these experiments, polymerization was initiated by exposure of the system to γ-rays; the relaxational kinetics were studied following the removal of the system from the radiation source. The results obtained for k_t were found to lie approximately within the upper and lower bounds predicted theoretically for residual termination.[7] In what follows, these relaxation experiments are extended to styrene. It is shown that styrene emulsion polymerizations display a different pattern of relaxation behavior from that of methyl methacrylate. To explain the novel results obtained, it has proved necessary to elaborate the concept, proposed by Cardenas and O'Driscoll[8] for bulk systems, that both entangled and unentangled free radicals can be involved in bimolecular termination events. In other words, it has proven necessary to use chain-length-dependent termination rate coefficients to describe the styrene emulsion polymerization kinetics that were obtained.

Experimental Section

The experiments performed were seeded emulsion polymerizations of styrene, the techniques for which have been described in detail previously.[11-14] Briefly, the results of a single experiment employing γ-radiation to initiate polymerization (see refs 11 and 12 for details) and three experiments using a chemical initiator (refs 13 and 14) are here reported. The conversion vs time curves were measured dilatometrically, all experiments being conducted at 50 °C. A monodisperse polystyrene latex of unswollen radius 179 ± 4 nm, as determined by electron microscopy, was used as a seed latex in all experiments. The initial concentration of monomer in the seed particles was 4.8 mol dm^{-3}, corresponding to interval III polymerization (i.e., to the absence of monomer droplets). The absence of secondary nucleation was confirmed by electron microscopy for all runs.

To obtain values of k_t as a function of w_p, successive relaxations were performed during a single run. Initiation was induced by γ-radiation from a ^{60}Co source at a dose rate of 25.6 mGy s^{-1}. The dilatometer remained exposed to the radiation at least until an essentially steady rate of polymerization was attained. The relaxation of the polymerization rate was monitored after subsequent removal of the dilatometer from the radiation field at least until an approximately steady rate was again achieved; the time required for removal is much shorter than the observed time scale for relaxation of polymerization. The dilatometer was then reinserted into the γ-radiation. This cyclic procedure was repeated until the conversion of monomer to polymer reached ca. 60%. In this way, values for k_t were determined over the w_p range 0.4–0.8. Some kinetic experiments were initiated by using potassium peroxydisulfate, as described elsewhere.[13,14]

Values of the average number of free radicals per particle ($\bar{n}$) were calculated from

$$\bar{n} = (dx/dt)/(k_p C_m N_c M_0/g_m{}^0 N_A) \quad (1)$$

where x = fractional conversion, k_p = propagation rate coefficient (taken[13] as 258 dm^3 mol^{-1} s^{-1}), C_m = concentration of monomer in the latex particles, N_c = seed latex particle number concentration, M_0 = molecular weight of the monomer, $g_m{}^0$ = initial mass of monomer, and N_A = the Avogadro constant.

Results and Discussion

One example of a conversion vs time curve for a series of relaxation runs over a range of w_p values is shown in Figure 1. Our first expectation was that conventional kinetic schemes (which do not take any possible chain-length dependence of rate parameters into account) could be used to fit such data. To do this, one proceeds as follows. To good approximation, the analysis of each relaxation curve can be assumed to correspond to one particular value of w_p. The general time evolution of $\bar{n}$ in an emulsion polymerization can be described by the Smith–Ewart equations.[13] However, as is shown in Figure 1, the pseudo-steady-state values of $\bar{n}$ prior to relaxation were typically greater than or equal to 2. Under these conditions, the Smith–Ewart equations can be approximated by the pseudo-bulk equation[11]

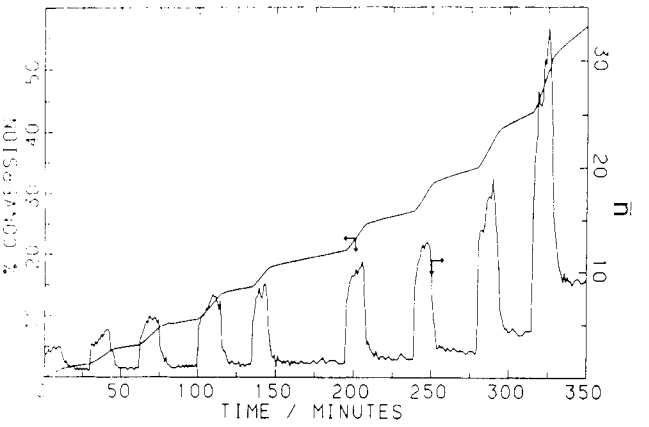

Figure 1. Conversion and $\bar{n}$ versus time curves for run GR100, showing the multiple insertions into, and removals from, the radiation source (number of latex particles = 3.5 × 10^{15} dm^{-3}, dose rate = 25.6 mGy s^{-1}; initial C_m = 4.8 mol dm^{-3}).

$$d\bar{n}/dt = \rho_a - (1 - \alpha)k\bar{n} - 2c\bar{n}^2 \quad (2)$$

where ρ_a = entry rate coefficient in the absence of exit, k = rate coefficient for exit (desorption) of free radicals, α = "fate parameter" (a dimensionless rate parameter accounting for the relative importance of reentry and aqueous-phase heterotermination of desorbed free radicals), and c = pseudo-first-order bimolecular termination rate coefficient; note that $c = k_t/(N_A V_s)$, where V_s = swollen volume of the latex particle. The second term in eq 2 can be neglected in these experiments on two accounts: first, the large particle size ensures that the value of k is small;[13] second, in relaxation experiments, the value of $\alpha \simeq +1$.[11] Accordingly, one expects

$$d\bar{n}/dt \simeq \rho_a - 2c\bar{n}^2 \quad (3)$$

Note that in relaxation experiments there is no primary source of free radicals so that the background thermal initiation alone is responsible for the radical generation; in these circumstances, ρ_a will be denoted by ρ_0. This thermal term is responsible for the nonzero pseudo-steady-state rate observed at long relaxation times (see Figure 1).

Through nonlinear least-squares fitting of the integrated form of eq 3 to the experimental $\bar{n}$ vs time relaxation data,[11] as illustrated in Figure 2, unique values of ρ_0 and c, and hence k_t, were obtained; these are listed in Table I. One difficulty that arises in such a treatment of the experimental data is that the empirical values of ρ_0 that must be used to obtain the requisite fits increase by over an order of magnitude as w_p increases from 0.48 to 0.74 (see Table I). Importantly, the fact that the ρ_0 values in Table I increase monotonically as w_p increases indicates that this increase is in fact a definite trend, not just an artifact of the fitting procedure. If the fitting procedure were such that some variation of ρ_0 about its optimum value could be endured without affecting the quality of the optimum

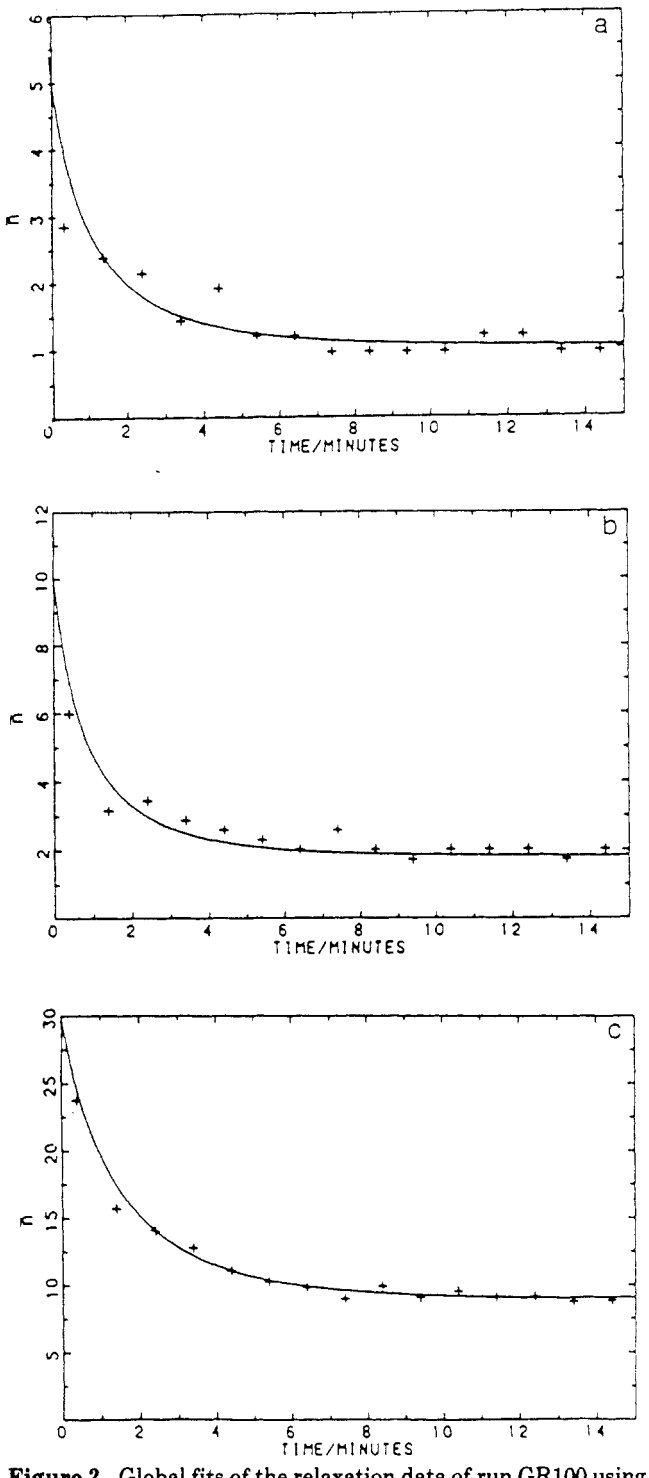

Figure 2. Global fits of the relaxation data of run GR100 using the pseudo-bulk equation; (a) $w_p = 0.51$; (b) $w_p = 0.60$; (c) $w_p = 0.74$. The experimental points are denoted by (+) and the theoretical fits using eq 3 by full lines.

fit too greatly, then some variation of ρ_0 from fit to fit would be expected. However, such a variation, being random, would shown no trend with w_p, which is contrary to the present experience, as noted above.

An alternative way of illustrating this trend of increasing ρ_0 with increasing w_p is presented in Figure 3, in which is plotted $d\bar{n}/dt$ vs $\bar{n}^2$ for two different relaxations. Before we explain the rationale behind such a plot, it should be noted that the fact that the out-of-source steady-state $\bar{n}$ values increase with w_p (a trend clearly apparent in Figure 1) is not necessarily a reflection of ρ_0 increasing with w_p. From eq 3 it is readily seen that this $\bar{n}$ value will be given by $(\rho_0/[2c])^{1/2}$; since k_t, and hence c, will decrease as w_p

Table I
Kinetic Parameters Determined from Relaxation Experiments (Run GR100 Using the Pseudo-Bulk Equation)

w_p	$10^3\rho_0/s^{-1}$	$10^4c/s^{-1}$	$10^{-4}k_t/dm^3\ mol^{-1}\ s^{-1}$
0.48	1.2	11	3.7
0.49	1.1	10	3.4
0.51	3.3	16	5.4
0.54	6.0	18	6.0
0.56	6.0	15	5.0
0.60	6.9	10	3.3
0.64	9.9	7.3	2.4
0.68	15	4.0	1.3
0.74	28	1.7	0.5

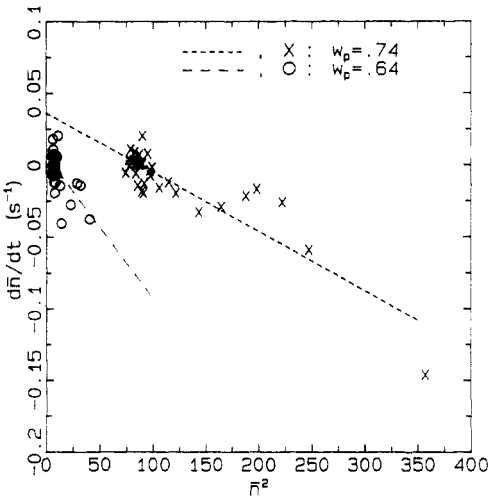

Figure 3. Plots of $d\bar{n}/dt$ versus $\bar{n}^2$ for run GR100 at $w_p = 0.74$ (×) and $w_p = 0.64$ (○). The lines are the least-squares fits to the data sets.

increases, it is clear that no increase in ρ_0 with w_p need necessarily be invoked to explain the increase in thermal $\bar{n}$ with w_p that was observed experimentally (see Figure 1). A more sophisticated means is therefore required to show that modeling of the experimental data of Figure 1 with the simplified pseudo-bulk equation, eq 3, must involve ρ_0 increasing with w_p, and this is what is achieved in Figure 3. Inspection of eq 3 reveals that the value of ρ_0 in this expression should be given by the intercept of such a plot with the $d\bar{n}/dt$ axis. The experimental scatter in such plots is quite large, as is expected for the second differential of noisy data. (It must be mentioned that the very initial points of the relaxation, being the most prone to noise, have been omitted from the present data analysis). Nevertheless, the intercepts obtained at different w_p are distinctly different. For example, least-squares linear fitting of the data presented in Figure 3 yielded intercepts of $(6.2 \pm 2.9) \times 10^{-3}$ and $(36 \pm 4) \times 10^{-3}$ s^{-1} for the relaxations at $w_p = 0.64$ and 0.74, respectively (the error values quoted are standard deviations). Thus it can be claimed with much confidence that the linear least-squares fits of the $d\bar{n}/dt$ vs $\bar{n}^2$ data for these relaxations do not have a common intercept, and this in turn is a persuasive indication that it is not possible to fit the data with a constant ρ_0 by using the current model. Before proceeding with the discussion, it is worth pointing out that the intercepts obtained by using the method of Figure 3 (these values should equal ρ_0) are very much in concordance with the fitted ρ_0 values reported in Table I, especially when the errors involved are taken into consideration.

It is thus established that, with the current method, fitting of the data is only possible with a ρ_0 that increases significantly, as noted above, with w_p. Such a dramatic increase in ρ_0 seems unlikely. Although the mechanism

by which thermal free radicals are generated in the emulsion polymerization of styrene remains unknown, it seems likely[14] that it is associated with the presence of the monomer-swollen latex particles, and perhaps with their surfaces. In the interval III experiments described here, there was a small decrease in particle size as monomer was converted into polymer. Both the decrease in particle size and the decrease in the monomer concentration in the system would point to a likely small decrease in ρ_0 as w_p increased, not an increase by an order of magnitude. Only if the products of γ-radiolysis were to act as catalysts for the thermal generation of free radicals would ρ_0 be expected to increase with increasing w_p. Such catalytic activity is not, however, observed at lower values of w_p in reinsertion experiments (see Figure 1 and Table I): the values of the thermal entry rate coefficient at lower w_p remain essentially unchanged with multiple insertions. This conclusion was confirmed by performing another experiment in which the initial charge of monomer was increased by 60% while holding the radiation dose rate constant. The values of ρ_0 thus obtained at comparable values of w_p were the same as those obtained from the experiment depicted in Figure 1.

The unphysical nature of the apparent increase in ρ_0 as w_p increases suggests that the simple interpretation of the experimental relaxation data in terms of eq 3 is erroneous. The difficulty with this simple model for relaxation can be further elaborated as follows. The thermally induced pseudo-steady-state observed at long times in the relaxation experiments allows the value of c to be calculated ($c = \rho_0/2\bar{n}_{SS}^2$, where the subscript SS refers to the steady state), provided that the value of ρ_0 is known. At lower w_p values, the value of ρ_0 was found experimentally to be essentially independent of w_p. If it is now assumed that this value is also applicable at higher w_p values for the reasons set forth above, c can be estimated from the long-time steady-state rate. The value of c so obtained can then be inserted into eq 3 to predict the decay of $\bar{n}$ at earlier times. A typical result, presented in Figure 4a, shows that the decay in $\bar{n}$ at early times predicted in this way is far too slow. Correspondingly, the theoretical conversion vs time curve lies well above the experimentally observed curve (see Figure 4b). This was true for all relaxation experiments where $w_p \gtrsim 0.6$. The experimental decay in $\bar{n}$ on relaxation always proved to be significantly faster than that expected from the long-time steady-state rate. Of course, agreement between the predicted and experimental values of $\bar{n}$ was obtained at longer times, but this is trivial and not shown in Figure 4a.

Inspection of the relaxation data (see Figure 1) shows that the approximate time taken to reach the thermally induced steady state increased only marginally with increasing w_p for $w_p \gtrsim 0.5$. This observation is in conflict, to some extent, with the expectation that bimolecular termination would be dominated by the residual mechanism at these w_p values. This is because the rate of residual termination is directly proportional to the monomer concentration, which decreases with w_p. Hence, if residual termination were rate determining, k_t would be expected to decrease with w_p, and consequently the relaxation times would be prolonged as w_p increased. It must be admitted that this phenomenon of the relaxation time being relatively insensitive to w_p is somewhat perplexing and not easily explained. At the very least it suggests the possible occurrence of more than one mechanism of bimolecular termination in the seeded emulsion polymerization of styrene. It was initially postulated that one of these mechanisms was dominant on a short time scale (up to a few minutes) whereas the other was dominant on a longer time scale (it will be shown subsequently that this postulate is incorrect). Such dual termination mechanisms are not incorporated into the Smith–Ewart formalism for particle growth in emulsion polymerization nor into the pseudo-bulk approximation thereof that has been used above. To interpret the experimental data obtained in these studies, it proved necessary to modify the pseudo-bulk equation to encompass additional mechanistic events.

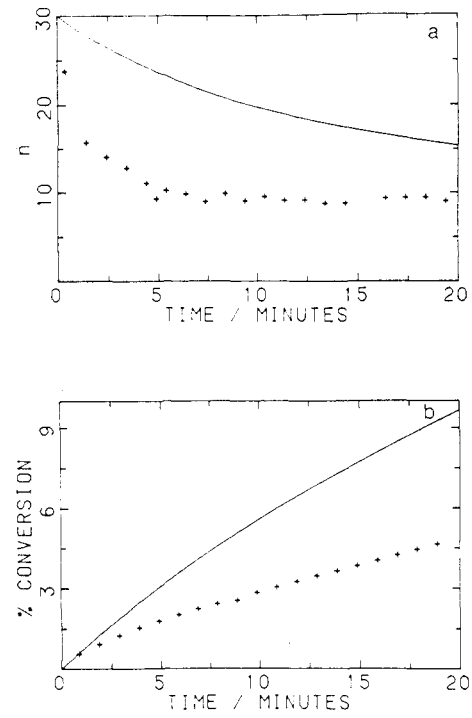

Figure 4. Plots of (a) $\bar{n}$ and (b) conversion versus time for run GR100 at $w_p = 0.74$. The experimental points are denoted by (+). The full lines are predicted theoretically by the pseudo-bulk equation, by using the value of k_t obtained at long times and the value of ρ_0 obtained at low w_p, viz., $c = 1.7 \times 10^{-6}$ s^{-1} and $\rho_0 = 3.0 \times 10^{-3}$ s^{-1}.

Modified Pseudo-Bulk Equation. The Short-Long Model. The modification in the Smith–Ewart model of latex particle growth that allows all of the kinetic data obtained in these studies to be explained in a consistent fashion is the extension to latex particles of the idea proposed for bulk systems by Cardenas and O'Driscoll.[9] It must be stressed that the model that will be elucidated here is not intended to mimic exactly the model of Cardenas and O'Driscoll just referred to (although we do follow the spirit of their concepts very closely). Rather, it is simply noted that both models stem from the same germinal idea, which is that of the presence of two subpopulations of free radicals: one consisting of free radicals attached to long, entangled polymer chains; the other of radicals attached to short, unentangled chains. The latter may arise from two distinct mechanistic events: first, the entry from the aqueous phase of styryl free radicals; second, chain transfer from long-chain free radicals to monomer molecules or chain-transfer agents. Long free radicals are formed by the propagational growth of the short chains to beyond some critical degree of polymerization necessary for entanglement.

Of course there will in reality be a wide range of free-radical chain lengths within the latex particles, and it is acknowledged that more complete modeling of these systems would more fully account for the entire distribution of free-radical chain lengths. In other words, the finite

difference approach adopted here, that of an arbitrary division into just two subpopulations, is clearly an oversimplification. This coarse graining will be shown, however, to be adequate for the purpose at hand. Radicals attached to either short or long chains may undergo bimolecular termination. Three different types of termination events may therefore be distinguished with this scheme: those between short chains (referred to as short–short termination), those between long chains (long–long termination), and those between a short chain and a long chain (short–long termination).

If $\bar{s}$ and $\bar{l}$ are the average number of radicals per particle attached to short and long chains, respectively, then the mechanistic events outlined above result in the following equations in the pseudo-bulk approximation

$$d\bar{s}/dt = \rho_a + k_{tr}C_m\bar{l} - k_pC_m\bar{s}/z - 2c_{ss}\bar{s}^2 - c_{sl}\bar{s}\bar{l}$$
$$d\bar{l}/dt = k_pC_m\bar{s}/z - k_{tr}C_m\bar{l} - c_{sl}\bar{s}\bar{l} - 2c_{ll}\bar{l}^2 \qquad (4)$$

where k_{tr} = rate coefficient for transfer to monomer, z = critical degree of polymerization at which short chains are deemed to become long chains, and the subscripts s and l refer to bimolecular termination events between species designated as short and long, respectively. These equations assume that transfer of short free radicals (which produces short free radicals) can be ignored; providing z is small relative to the overall average chain length of polymer that is formed, this is reasonable. It is also assumed, in the absence of any other information, that entering species are short free radicals; it certainly seems unlikely that newly generated free radicals would be long and entangled. Note that the foregoing equations are only applicable when chain transfer is confined to monomer and when $\bar{n}$ $(=\bar{s} + \bar{l}) \gtrsim 2$. Chain transfer to added chain-transfer agents (CTA) is readily incorporated by the appropriate inclusion of terms of the form $k_{tr}[CTA]\bar{l}$. Note also that the overall rate of conversion of monomer to polymer is still given by eq 1. Note further that ρ_a equals ρ_0 for relaxation conditions.

Equation 4 displays a proliferation of rate coefficients in comparison with eq 3. Using these equations to model our experimental data may therefore at first seem to be a measure incompatible with our stated aim in carrying out this work: to extract, without prejudice, meaningful termination rate coefficients from the experimental data and to invoke as few model-based assumptions as possible in doing so. As an advance assurance that this incompatibility not be the case, the results of our data analysis will now be summarized before presentation of this analysis. It transpires, as will be shown, that eq 4 really contains no more effective parameters than eq 3; the parameters that turn out to be of importance are $k_{t,sl}(w_p)$ and ρ_a (which is independent of w_p). By fitting of eq 4 to the experimental data alone and introducing only a bare minimum of model-based assumptions in doing so, we shall obtain $k_{t,sl}(w_p)$. Finally, the rectitude of this approach and the values so procured will be supported by the presentation of a molecular level theory, which will be seen to yield the same values (within experimental uncertainty) for $k_{t,sl}(w_p)$ without reference to any of the kinetic data.

We now proceed with the data analysis in detail. As already noted, eq 4 displays a seeming plenitude of parameters in comparison to eq 3. Fortunately, it proved possible to reduce some of the arbitrariness of the data analysis by providing estimates of certain of the rate coefficients. This reduces the number of adjustable parameters when fitting the experimental data. Thus, the value of c_{ll} can reasonably be constrained to lie within the flexible- and rigid-chain limits proposed by Russell et al.[7] for residual termination. The value of k_{tr} ($=6 \times 10^{-3}$ dm^3 mol^{-1} s^{-1}) was taken from the literature,[15] although it must be admitted that the precision of this value is unlikely to be better than ±50%. The entanglement spacing of pure polystyrene has been measured[16] as being about 180 monomer units; for this reason the value z = 180 was used in the present modeling. An additional constraint adopted in the preliminary data analyses was that ρ_0 must be independent of w_p over the range studied, although this constraint ultimately proved to be unnecessary. Finally, the cross-termination rate coefficient c_{sl} can be set equal to c_{ss} to good approximation. The reason for this is as follows. Equation 4 follows the IUPAC recommendation[17] with regard to use of stoichiometric coefficients in defining the rates of bimolecular termination events. Now, at the w_p of these experiments all termination events will be diffusion controlled and thus must obey the Smoluchowski equation: $k_t = 4\pi N_A Dr$, where D is an appropriate diffusion coefficient and r is an appropriate capture radius for reaction. However, the IUPAC convention requires for consistency that the Smoluchowski equation be written in two different forms for diffusion-controlled termination processes according to whether or not the mutually annihilating species are of the same subpopulation. Thus, $k_{t,sl} = 4\pi N_A(D_s + D_l)(r_s + r_l)$ whereas $k_{t,ss} = 2\pi N_A(D_s + D_s)(r_s + r_s)$, where D is the self-diffusion coefficient of the radical species and r is its radius of interaction. Now, the long chains are bulkier than short chains, and, further, it is envisaged that the long chains are entangled whereas the short chains, by and large, are not similarly restrained; hence, $D_l \ll D_s$. Moreover, since the actual free-radical chain end is the same size whether or not the chain itself is short or long, the radius of interaction for short–long termination, $r_s + r_l$, should closely approximate the radius of interaction for short–short termination, $r_s + r_s$. Given both of these approximations, it follows that $k_{t,sl} \simeq k_{t,ss}$ and the corresponding values of c can also be set equal.

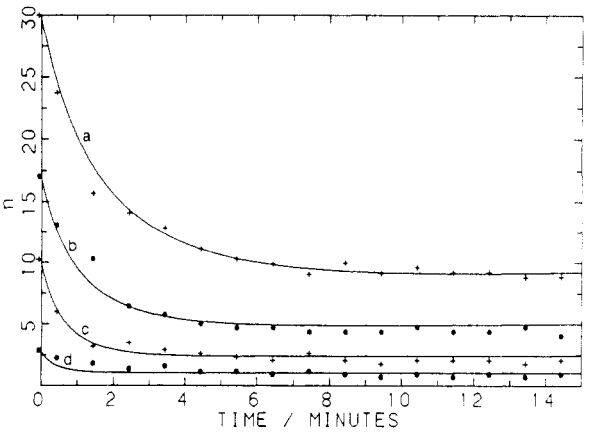

Figure 5. Comparison of the predictions of the short–long model (full lines) with the experimental free-radical decay points for some relaxations of run GR100; w_p values: (a) 0.74, (b) 0.68, (c) 0.60, and (d) 0.48.

The foregoing discussion implies that virtually only two parameters (ρ_0 and c_{sl}) in eq 4 are arbitrarily adjustable when fits are made of eq 4 to the experimental relaxation data. Some of these fits are shown in Figure 5. These fits were generated on a computer by using the Gear algorithm to integrate eq 4 numerically. Only a relatively narrow range (±25%) of values for the pair of parameters ρ_0 and c_{sl} were found to describe adequately each set of experimental results. Initially, the value of ρ_0 was constrained to be independent of w_p, but this proved to be unnecessary because ρ_0 was found to behave in this way when this

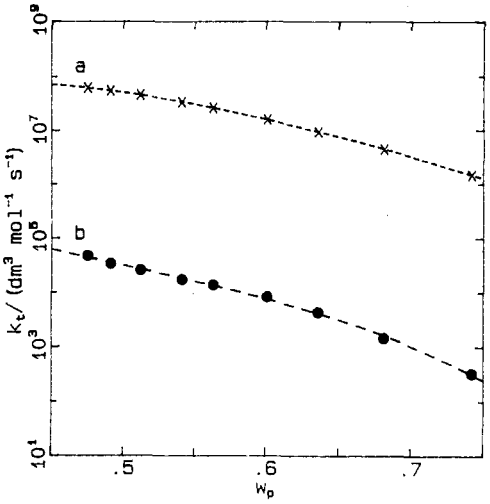

Figure 6. Dependence of the termination rate coefficients on the weight fraction of polymer, w_p, calculated from run GR100 by using the short–long model: (a) short–long coefficient $k_{t,sl}$; (b) long–long coefficient $k_{t,ll}$; points, values calculated from experiments; lines, cubic polynomials of best fit (quoted in text) for these sets of points.

constraint was removed.

The numerical values obtained for $k_{t,sl}$ ($=k_{t,ss}$) and $k_{t,ll}$ as a function of w_p are presented in Figure 6; these values were obtained by using $0.016\ s^{-1} \leq \rho_0 \leq 0.040\ s^{-1}$. Note that $k_{t,sl}$ is three to four orders of magnitude larger than $k_{t,ll}$. The following empirical expressions were found to model the experimental results over the range $0.48 \leq w_p \leq 0.75$:

$$\log k_{t,sl}/\mathrm{dm^3\ mol^{-1}\ s^{-1}} = 4.4982 + 19.621w_p - 32.655w_p^2 + 12.456w_p^3$$

$$\log k_{t,ll}/\mathrm{dm^3\ mol^{-1}\ s^{-1}} = 13.636 - 42.615w_p + 72.398w_p^2 - 47.441w_p^3$$

Note, however, that the solutions to eq 4 are insensitive to the value of $k_{t,ll}$ and so no great reliance can be placed on the values obtained by this method. For example, the following parameter set was used in the simulation, depicted as curve a in Figure 5, of the relaxation at $w_p = 0.74$: $\rho_0 = 0.04\ s^{-1}$, $z = 180$, $k_{t,sl} = 1.47 \times 10^6\ dm^3\ mol^{-1}\ s^{-1}$, and $k_{t,ll} = 3.23 \times 10^2\ dm^3\ mol^{-1}\ s^{-1}$. If $k_{t,ll}$ was set equal to zero and the same values of z and ρ_0 were retained, it was found that the data could be fitted equally well with $k_{t,sl} = 1.62 \times 10^6\ dm^3\ mol^{-1}\ s^{-1}$. On the other hand, if $k_{t,ll}$ was increased by an order of magnitude from the original value and set equal to $3.23 \times 10^3\ dm^3\ mol^{-1}\ s^{-1}$, then the data could be well modeled with $k_{t,sl} = 8.40 \times 10^5\ dm^3\ mol^{-1}\ s^{-1}$. What this illustrates is that the value of $k_{t,ll}$ is relatively unimportant in the modeling; the quoted values of $k_{t,ll}$ should be treated as being accurate to within no more than an order of magnitude; however, the value of $k_{t,sl}$ is relatively insensitive to even order of magnitude variation of $k_{t,ll}$, and consequently the values of $k_{t,sl}$ can be regarded with some confidence as being reliable.

As is intimated in the above discussion, the present model reveals short–long termination to be the dominant mode of termination in these systems. Again, this is well illustrated by the $w_p = 0.74$ relaxation, for which it was found that, with $k_{t,ll}$ and $k_{t,ss}$ both set equal to zero and with ρ_0 and z as above, a value of $k_{t,sl} = 1.65 \times 10^6\ dm^3\ mol^{-1}\ s^{-1}$ could successfully reproduce the experimentally observed kinetics. In fact, all relaxations could be modeled as successfully in this fashion as with any fuller parameter set (within the scope of the present model). This shows conclusively that this model, despite all the variables in the eq 4, really is a two-parameter model as earlier claimed. It is important to recognize, however, that this does *not* make this model equivalent to the more basic pseudo-bulk model. If one puts $c_{ll} = c_{ss} = 0$ in eq 4, then these equations reduce to

$$d\bar{n}/dt = \rho_a - 2c_{sl}\bar{s}\,\bar{l} \tag{5}$$

where $\bar{s}$ and $\bar{l}$ must obviously be defined (and interrelated) by some other equation(s). The point here is that although eq 5 has the same form as eq 3, it is clear that the two equations differ fundamentally in their termination terms: eq 5 cannot be reduced to a single second-order differential equation of the form of eq 3. Equation 5 emphasizes why the short–long model is able to model more completely and consistently the entire body of relaxation data than eq 3: it is not because there are more adjustable parameters in the short–long model (from the above discussion, it is apparent that this is not the case); rather, it is because the short–long model more accurately pinpoints the termination mechanism that it is able to account better for the experimental data.

The encouraging agreement between experiment and theory aside, it must be stressed that even the value of $k_{t,sl}$, the most important parameter in the model, is model dependent. Once again the relaxation at $w_p = 0.74$ is used to exemplify this. It may be suggested that a value of $z = 100$ be used to model the data; this is a reasonable suggestion, first, on the grounds that z should decrease with w_p (increasing dilution of the polymer will act to increase the entanglement spacing of the polymer, so if $z = 180$ at $w_p = 0.48$, then a lower z should be used at higher w_p), and, second, because the value of z is by no means clear-cut in the first place. With this lower value of z and with ρ_0 and $k_{t,ll}$ as used in producing Figure 5a, it was necessary to set $k_{t,sl} = 2.75 \times 10^6\ dm^3\ mol^{-1}\ s^{-1}$ to reproduce (without any loss of quality in comparison to other fits) the experimental data, as compared to the value $1.47 \times 10^6\ dm^3\ mol^{-1}\ s^{-1}$ above. Thus, while $k_{t,sl}$ is somewhat model dependent, this dependence is not so strong as to undermine its significance or impugn its order of magnitude value.

The calculations of the above paragraph are also important from another viewpoint. It might be quite reasonably suggested that in this model z should be a function of w_p rather than being set independent of w_p. For example, there is some evidence,[16] both theoretical and experimental, that z is inversely proportional to the volume fraction of polymer. If this were the case, then z would increase by a factor of approximately $0.75/0.50 = 1.5$ as w_p decreased from 0.75 to 0.50, this being the range of w_p spanned by the relaxation experiments under consideration. However, the results of the above paragraph clearly indicate that increasing z by 50% in modeling $w_p \approx 0.5$ relaxations will alter the value obtained for $k_{t,sl}$ by a factor of 2 at most. When it is recognized that the $k_{t,sl}$ obtained here by modeling varies by nearly 2 orders of magnitude over the w_p range investigated (see Figure 6), it is quickly concluded that any reasonable scaling of z with w_p would barely affect the $k_{t,sl}(w_p)$ obtained in comparison with that obtained with a constant z. It is also noteworthy that the uncertainty in the value of z for pure polymer, as already mentioned, is in itself greater than the variation in z with w_p that one might reasonably expect in passing from $w_p = 0.48$ to $w_p = 0.74$. An undue emphasis on such a variation therefore seems inappropriate, although it is acknowledged that, strictly speaking, the variation of z with w_p should be incorporated into the present kinetic model.

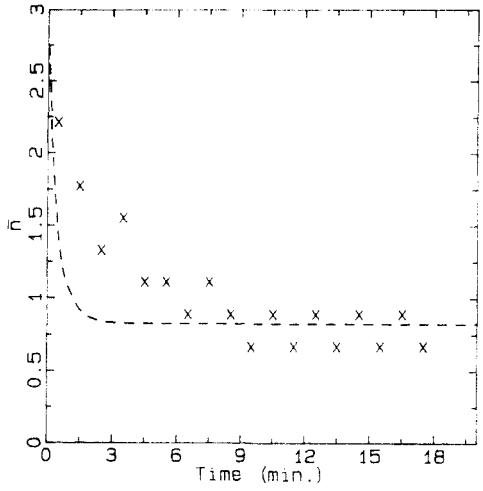

Figure 7. Plot of $\bar{n}$ versus time for run GR100 at $w_p = 0.48$. The experimental points are denoted by (×). The line is that fitted by the short–long model.

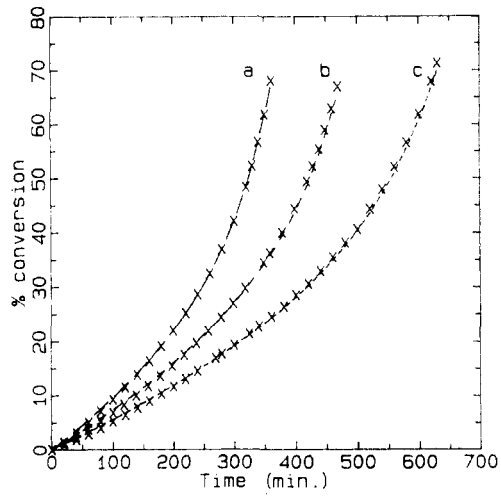

Figure 8. Comparison of the predictions of the short–long model (full line) with the experimental conversion versus time points for chemically initiated seeded emulsion polymerizations of styrene. $[K_2S_2O_8]$: (a) 9.9×10^{-4}, (b) 5.5×10^{-4}, and (c) 1.5×10^{-4} mol dm^{-3}, ρ_a: (a) 0.133, (b) 0.08, and (c) 0.035 s^{-1}.

It should be noted that the model shows that the fraction of the free-radical population in the latex particles that is unentangled is always small (typically, $\bar{s}/\bar{n}$ is of the order of 0.5% with $z = 180$). As has already been made clear, despite this relatively small population of short chains, it is the termination events between free radicals attached to short and long chains that dominate bimolecular termination (the $c_{sl}\bar{s}\bar{l}$ terms in eq 4). Residual termination between long chains (the $2c_{ll}\bar{l}^2$ term) is relatively unimportant because c_{ll} is so much smaller than c_{sl}. Termination between two short chains (the $2c_{ss}\bar{s}^2$ term) is also relatively unimportant because $\bar{s}$ is small compared with $\bar{l}$ and $c_{ss} = c_{sl}$. Indeed, the rate of short–short termination is usually the smallest of the three bimolecular termination processes considered.

It is instructive to ascertain the mechanistic reasons for the small population of short chains. The answer resides in the relative rapidity of propagation of short chains to beyond their critical length for entanglement, compared with the characteristic times of other kinetic events. Consider a typical latex particle polymerizing in source just prior to relaxation. Suppose $C_m = 2.5$ mol dm^{-3} (i.e., $w_p \simeq 0.74$); then the time it takes for a short chain to propagate to its entanglement length is $z/(k_pC_m) \simeq 0.3$ s at most. Typically, under these conditions, the short–long model requires for agreement between theory and experiment that $\bar{s} \simeq 0.21$, $\bar{l} \simeq 30$, $c_{sl} \simeq 0.0455$ s^{-1}, and $\rho_a \simeq 0.6$ s^{-1}. This implies that, on average, short free radicals would appear in a latex particle as a result of entry about every 2 s, an interval similar to that $[1/(k_{tr}C_m\bar{l}) \simeq 2$ s] between the production of short free radicals by chain transfer to monomer. In addition, a short–long bimolecular termination event occurs in a particle every 3.5 s $[\simeq 1/(c_{sl}\bar{s}\bar{l})]$ on average. What these calculations show is that the time required for propagational growth of short chains to the entanglement length is short compared with the time scales for either their bimolecular termination or the interval between their production. Such conditions necessarily presage that $\bar{l} \gg \bar{s}$.

A final point that must be made in regard to the modeling of these relaxations is that the model of eq 4 describes the experimental results far better when $\bar{n}$ is high (the high w_p relaxations). This is illustrated in Figure 7, in which are presented the results of modeling of the $w_p = 0.48$ relaxation with parameters as in Figure 5. It is clear that the model accounts for the thermal steady-state accurately but is inadequate in describing the initial relaxation from the in-source steady state: the simulated decay in $\bar{n}$ is far more rapid than is experimentally observed. Why the model should suffer from this shortcoming is not immediately obvious and is the subject of ongoing investigation. This difficulty is a manifestation of a problem that has been already mentioned: that of why the time taken to pass from an in source to an out-of-source pseudo-steady-state is relatively insensitive to the value of w_p.

A further test of the validity of the short–long interpretation of the relaxation data is whether the values derived therefrom can be used to model kinetic results obtained with chemically initiated systems. Admittedly, the entry rate coefficient in eq 4 represents an unknown adjustable parameter that allows the fit of the theoretical model to the experimental data to be optimized. However, the actual shape of the simulated conversion vs time curves is determined not so much by ρ_a as by the dependences of the termination rate coefficients on w_p, variations which are fixed by the relaxation results. Figure 8 illustrates the excellent agreement that can be achieved between theory and experiment for chemically initiated systems. Moreover, the values of ρ_a obtained in this way (refer to Figure 8) are consistent with those that would be predicted theoretically for entry into the relatively low concentration of large particles that were studied here.[18] The apparent ability of the short–long model to explain both chemically initiated runs and relaxation experiments points to its essential rectitude. In view of the difficulties associated with low w_p modeling that were mentioned above, it might at first appear surprising that eq 4 can, with parameters from the relaxation modeling, so successfully simulate the low w_p kinetics from the chemically initiated experiments. However, given that the relaxation modeling sought, and managed, to model at least the thermal steady state, it becomes apparent why the modeling of the chemically initiated experiments was successful: in these experiments a pseudo steady state reigns—there are no disruptions, such as removal from exposure to a source of γ-radiation, to perturb the system drastically. A further point to mention is that, as with the relaxation experiments, short–long termination predominated in the modeling of the chemically initiated experiments, and these experiments could be equally well modeled by retaining the same $k_{t,sl}(w_p)$, setting $k_{t,ss} = k_{t,ll} = 0$, and making only a slight alteration to ρ_a.

An additional check on the reasonableness of the short–long model is whether the average distance between the entangled free radicals is less than the distance that the unentangled free radicals can diffuse before growing to the critical entanglement length. Unless this inequality is obeyed, the model would have to be discarded. Taking the data corresponding to $w_p = 0.74$ by way of example: the swollen volume of the latex particles at this w_p was 5.4×10^{-17} dm^3. The lowest value of $\bar{l}$ during the course of the relaxation is that of the thermal steady state, viz., $\bar{l} \simeq 10$. Assuming a uniform distribution of these entangled free radicals, their maximum separation was thus of the order 175 nm. It is possible to set upper and lower bounds for the distance a short free radical may diffuse before entanglement. It was shown above that the time taken for growth to the entanglement length under these conditions is about 0.3 s. The Einstein equation, $\langle r^2\rangle^{1/2} = (6Dt)^{1/2}$, allows the mean diffusion distance in this time to be calculated if D is known. The largest value that D can adopt under these conditions is that corresponding to monomer at this value of w_p. Although the value of D for styrene at this w_p has not apparently been measured, the value for another relatively small molecule, hexafluorobenzene, has been determined to be of the order 4×10^{-8} cm^2 s^{-1} at $w_p \simeq 0.71$ at 30 °C.[19] This value is certainly a lower bound for the diffusion coefficient at this w_p of the smaller styrene molecule at the higher temperature of 50 °C; it will be adopted here as only an order of magnitude is required. It yields $\langle r^2\rangle^{1/2} \simeq 2700$ nm, an upper limit to the diffusional distance of a short chain prior to entanglement. The smallest value that D seems likely to adopt is that of the unentangled polymer coil immediately prior to entanglement. The effective "diameter" of a polystyrene coil of critical degree of polymerization 180 can be calculated from[20] $d_{chain} \simeq (C_\infty)^{1/2}\lambda n^{1/2}$, where C_∞ = characteristic ratio of polystyrene (=7.0),[20] λ = C–C bond length (0.154 nm), and n = number of C–C bonds in the backbone. The effective radius is thus 3.9 nm; note that this is a maximum coil size—the radius of gyration, which can be (especially for small chains) the more appropriate quantity to use in the Stokes–Einstein equation below, will be somewhat less than this. In the absence of entanglements, the Stokes–Einstein equation suggests that $D_{chain} \simeq D_{HFB}d_{HFB}/d_{chain}$, where $d_{HFB} \simeq 0.26$ nm (calculated from its density and assuming spherical geometry; this is undoubtedly an underestimate of d_{HFB}). This yields $D_{chain} \simeq 1 \times 10^{-9}$ cm^2 s^{-1}, corresponding to a diffusional distance before entanglement of the order of 500 nm. Thus, both the upper (2700 nm) and lower (500 nm) bounds for the diffusional distance before entanglement substantially exceed the distance (175 nm) between entangled free radicals. Although these calculations are very approximate, they nevertheless emphatically suggest not just that short–long termination is possible but that it is indeed likely to occur. Similar calculations performed at lower values of w_p, at which D values will be even higher, favor the occurrence of short–long termination to an even greater extent.

Theoretical Model for the Short–Long Termination Rate Coefficient. In this section we endeavor to calculate $k_{t,sl}$ from first principles and to compare the values so obtained with those derived from experiment. Prediction of $k_{t,sl}$ proceeds from the Smoluchowski equation:

$$k_{t,sl,diff} = 4\pi N_A(D_s + D_l)(r_s + r_l) \quad (6)$$

The terms in this equation have already been defined; note that the subscript "diff" denotes that eq 6 specifies the diffusional contribution to $k_{t,sl}$. In eq 6, a good estimate of the radius of interaction for short–long termination is the Lennard-Jones diameter of a monomer unit, here signified as σ. Since long chains are bulky and entangled, their center-of-mass diffusion will be slow; it seems reasonable to assert, therefore, that diffusion of the long free-radical chain-end will be determined by the rate of propagation at this site. One thus has[7]

$$D_l = k_pC_ma^2/6 \quad (7)$$

where a is the root-mean-square end-to-end distance per square root of the number of monomer units of the polymer. Equation 7 is certainly a lower bound for D_l; in the present calculations it transpires that D_l is negligible in comparison to D_s, which is as intuitively expected.

The quantity D_s is not so readily specified, primarily because D_s does not pertain to a particular species; rather, D_s represents an average diffusion coefficient for a whole series of oligomeric free radicals. As such, D_s is best defined with reference to the Einstein relation:

$$D_s = \langle R_s^2\rangle/(6t_s) \quad (8)$$

Here $\langle R_s^2\rangle$ is the mean-square displacement of a short free radical in its lifetime t_s. Since short species are predominantly generated by transfer, this lifetime is simply the time taken for a monomeric free radical to grow, by propagation, into a long free radical. Given this, the overall distance diffused by a short species must be the sum of the distances it diffuses at each successive stage (as an i-meric free radical) of its life:

$$\langle R_s^2\rangle = \sum_{i=1}^{z}\langle R_i^2\rangle = \sum_{i=1}^{z}6t_iD_i \quad (9)$$

Here $\langle R_i^2\rangle$ is the mean-square displacement of an i-mer, with diffusion coefficient D_i, during its lifetime t_i. Implicit in eq 9 is the notion that a short species becomes a long (entangled) chain at degree of polymerization z, a quantity that thus may be thought of as marking a degree of polymerization at which some qualitative change in the nature of the diffusion of the free-radical chain occurs. In the absence of any more specific information, the reasonable assumption that the rate of propagation is chain length independent is made; therefore, $t_i = 1/(k_pC_m)$, and hence $t_s = z/(k_pC_m)$. Finally, there is some evidence[21] that the diffusion coefficients of low molecular weight (unentangled) polymer species in concentrated polymer solutions scale as the reciprocal of the molecular mass of the species. This result implies that $D_i \simeq D_m/i$, where D_m is the diffusion coefficient of a monomeric free radical. Combining the results of this paragraph so far yields:

$$D_s = \frac{D_m}{z}\sum_{i=1}^{z}\frac{1}{i} \quad (10)$$

Equation 10 and the other results of this section lead to:

$$k_{t,sl,diff} = 4\pi N_A\sigma\left(\frac{k_pC_ma^2}{6} + \frac{D_m}{z}\sum_{i=1}^{z}\frac{1}{i}\right) \quad (11)$$

It is noted that the summation in eq 11 can be well approximated by an integral from $i = {}^1/_2$ to $i = z + {}^1/_2$, so yielding the result:

$$k_{t,sl,diff} = 4\pi N_A\sigma\left[\frac{k_pC_ma^2}{6} + \frac{D_m \ln(2z+1)}{z}\right] \quad (12)$$

This expression is useful for quick evaluation; however, the more exact eq 11 is used for calculations in the present instance.

A complete formulation for $k_{t,sl}$ must account for the short–long termination event involving both a diffusion step and an encounter step. The usual procedure with regard to the latter is to assume that the rate of segmental motion of the polymer chain units is chain length independent; certainly this assumption should not be too awry in considering the shortest time scale motions of a monomer unit within a chain of any significant length (say, one of degree of polymerization 10). As a first approximation one therefore uses a value $k_{t,o}$ as an umbrella term for describing the rate of segmental termination for species of all chain lengths. In the standard fashion, one then puts[9,22]

$$1/k_{t,sl} = 1/k_{t,o} + 1/k_{t,sl,diff} \quad (13)$$

Equation 13 is the required expression for the short–long termination rate coefficient.

In using eqs 11 and 13 to calculate $k_{t,sl}$, the following values were used: $\sigma = 0.602$ nm,[7] $a = 0.74$ nm,[7] and $k_{t,o} = 4.98 \times 10^7$ dm^3 mol^{-1} s^{-1}.[23] This value of $k_{t,o}$ is the value of k_t derived from very low conversion (under which conditions segmental diffusion is thought to be the rate-determining termination step) bulk polymerization of styrene. In actuality, the segmental motions of the polymer chains will be affected by w_p, and so $k_{t,o}$ will vary with w_p, but this is an area that, to the best of our knowledge, remains uninvestigated at the high weight fractions that we are considering here. Consequently, this low conversion $k_{t,o}$ value is taken as being applicable here, and further it is assumed to be w_p independent. In passing, it is suggested that intuition dictates that this value of $k_{t,o}$ is an upper bound for the actual value at the w_p values of interest here. An approximate variation of D_m with w_p was obtained from experimental measurements of D for methyl red in polystyrene at 50 °C.[24] The following cubic polynomial, obtained by least-squares fitting, provided an excellent fit to this data over the range $0.4 \leq w_p \leq 0.7$ (no measurements are reported for $w_p \geq 0.7$):

$$\log D/\text{cm}^2\ \text{s}^{-1} = 0.4170 - 29.51w_p + 53.14w_p^2 - 36.03w_p^3 \quad (14)$$

In the absence of any data more germane to the purpose at hand, the above expression was adopted for specifying D_m as a function of w_p over the range $0.48 \leq w_p \leq 0.74$, this being the range of w_p over which relaxation experiments were carried out. Finally, the value of z must be taken as 180, for it was this value that was used in deriving the "experimental" values of $k_{t,sl}$ against which the calculated values of $k_{t,sl}$ are to be compared.

A comparison between the predicted values of $k_{t,sl}$ and those observed experimentally is presented in Figure 9. It is clear that the method of this section succeeds admirably in predicting the experimentally observed $k_{t,sl}$, especially in view of both the theoretical approximations and data specification limitations involved. This agreement between experiment and theory provides added impetus for regarding the short–long interpretation of termination that is presented in this paper as being fundamentally correct. Further, the calculations of this section suggest that some degree of confidence may be warranted with regard to the prospect of eventual a priori modeling of termination throughout the industrially important middle reaches of polymerization.

Origin of the Trommsdorff–Norrish Gel Effect in These Systems. Bimolecular termination processes are involved in the well-known phenomenon that is commonly referred to as the Trommsdorff–Norrish,[25,26] or gel, effect. It is generally agreed that the autoacceleration observed

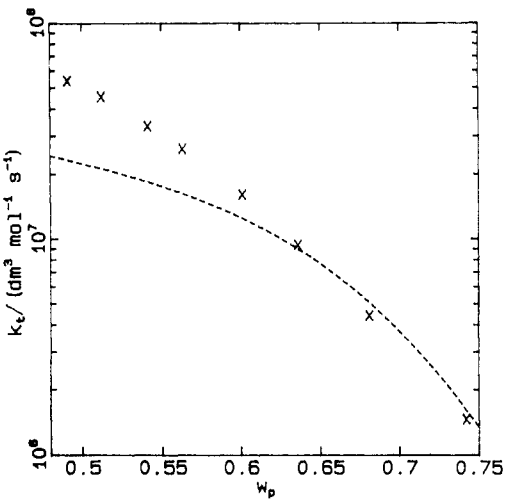

Figure 9. Comparison of values of the short–long termination rate coefficient, $k_{t,sl}$: line, values calculated by using eqs 11 and 13; points, values derived (by using the short–long model) from experiments.

in certain bulk polymerizations once some polymer has been formed has its origins in the reduction in the termination rate coefficient that occurs as the weight fraction of polymer in the system increases. However, precise identification of the mechanistic processes responsible for this reduction has proved to be difficult. Dionisio et al.[22] postulated that the change in the rate-determining step for radical termination from segmental diffusion to translational diffusion of the polymer coils was responsible for the occurrence of the gel effect. This explanation is unlikely to have widespread validity because the onset of autoacceleration is often observed at polymer concentrations significantly higher than those concentrations corresponding to the onset of coil overlap and chain entanglement. Turner[27] proposed that the onset of the gel effect corresponds to the achievement of close packing of macromolecules with unperturbed dimensions. Balke and Hamielec[28] have invoked a change in the free volume of the system as the cause of autoacceleration. Tulig and Tirrell[3] developed a theory that ascribes the onset of the gel effect to reptative motion of the entangled macroradicals becoming the dominant contributor to center-of-mass diffusion (this would be of order c^{**} in the de Gennes scaling theory[29]). Note, however, that, in a recent review, Mita and Horie[1] have concluded that "the relationship between the onset of the gel effect and the onset of the entangled behavior in rheological properties is still unclear." It is by no means even clear that the gel effect is the result of a single physical phenomenon: the autoacceleration in rate that is the signature of the gel effect may very well stem from different effects in different systems or from the interplay of several different phenomena.

The theoretical conversion versus time curves shown in Figure 8 apparently exhibit autoacceleration that commences at $w_p \simeq 0.6$. Thus the short–long model is able to predict the occurrence of the Trommsdorff–Norrish gel effect in these seeded emulsion polymerizations of styrene. It was mentioned previously that the most widely accepted explanation for the onset of autoacceleration in bulk systems was the marked reduction in k_t due to chain entanglements. This explanation at first sight seems unlikely to be valid for the emulsion polymerizations studied here because the high molecular weight chains generated would become entangled at w_p values significantly below 0.6. It must be recognized, however, that the ultimate molecular weight to which the chains grow

does not necessarily determine the critical value of w_p required for the onset of rate acceleration. Rather, the foregoing model suggests that the onset of the gel effect may well be related to the point at which some shorter free-radical species becomes entangled; specifically, this critical chain length may be the minimum degree of polymerization z necessary for entanglement. Given this, the occurrence of a gel effect at $w_p \simeq 0.6$ becomes more readily comprehensible.

A simpler, alternative explanation for the occurrence of the autoacceleration follows from the short–long model. Inspection of the numerical data calculated by the short–long model for the various microscopic kinetic events that generate, terminate, and interconvert the two different types of free radicals does not reveal any dramatic changes in their values at $w_p \simeq 0.6$. There does, however, appear to be an exponential increase, at this w_p, in the rate of production (i.e., $d\bar{s}/dt$ in eq 4) of short free radicals, which, as a result of growth, are quickly transformed into long free radicals. These processes are, of course, present in the system right from the commencement of the seeded polymerizations, but their kinetic manifestation in the form of a strong autoacceleration is only apparent at $w_p \simeq 0.6$. The shape of the plot of log $k_{t,sl}$ vs w_p (see Figure 6), which is concave to the w_p axis, favors this type of behavior; as expected, this curve resembles in general form the dependence on w_p of the logarithm of the diffusion coefficient of low molecular weight species in polystyrene.[30,31] Such diffusion presumably occurs by a free volume mechanism. As monomer is consumed, the formation of the requisite free volume to allow diffusion to occur becomes increasingly more difficult, thus generating the observed concave shape of the relevant diffusion coefficient curve. The implication of this for polymerization kinetics is as follows: as the monomer diffusion coefficient drops, so too will $k_{t,sl}$. This means that more short species will survive to become long species so that $\bar{n}$ increases and so acceleration in rate results. The gel effect seen in these systems is thus postulated to result from the monomer diffusion coefficient beginning to decrease at an accelerating rate with increasing w_p.

Conclusion

It was found by using large seed latex particles polymerizing in interval III that the relaxation processes in styrene emulsion polymerizations differ significantly from those of methyl methacrylate. Whereas bimolecular termination in methyl methacrylate emulsion systems is apparently dominated by residual termination between entangled chains,[7] the relaxation results in styrene systems display more complex patterns of behavior. These have been successfully interpreted in terms of a short–long model that postulates the existence of two subpopulations of free radicals: those attached to short mobile chains and those attached to long entangled chains. The latter are formed by the rapid propagational growth of the former so that the population of the long chains is relatively large compared with that of the short chains. The short chains are generated by free-radical entry and by chain transfer. Although their relative concentration is small, the diffusional mobility of the small chains is so great that mutual termination between pairs of the free radicals attached to short and long chains, respectively, constitutes the major mechanism of free-radical annihilation. The short–long model derived from the relaxation studies is able to describe the shape of the kinetic curves obtained by using chemical initiation, including the onset of the Trommsdorff–Norrish autoacceleration. Despite their apparent complexity, the short–long equations in fact contain only two adjustable parameters, no more than in the original pseudo-bulk equations that do not differentiate between chain lengths. An important feature of the work of this paper is that a molecular level model for the short–long termination rate coefficient has been derived. This model uses observed diffusion coefficients and successfully reproduces the experimental rate parameters, which strongly suggests the correctness of both the data interpretation and the theoretical model.

Finally, it is worthy of mention that the short–long model undoubtedly grossly simplifies the actual nature of these systems. For example, the short–long model does not fully account for the entire distribution, in all its complexity, of free radicals that are present in these systems nor does it admit the possibility of spatial inhomogenieties within the latex particles. These shortcomings are obvious subjects for continuing research in this area. Also, it must be emphasized that γ-relaxation experiments, because they entail polymerizing systems passing from one pseudo-steady-state to another, are a far more sensitive test of mechanistic assumptions than traditional steady-state initiation experiments. Experiments of the former type are therefore strongly recommended for the purpose of testing models of polymerization kinetics.

Acknowledgment. The support of the Australian Research Council and the Australian Institute of Nuclear Science and Engineering, the provision of facilities by the University of Sydney Electron Microscope Unit, and Commonwealth Postgraduate Research Awards for M.E.A. and G.T.R. are all gratefully acknowledged. Mr. G. R. Baxter of the CSIRO Division of Chemicals and Polymers is thanked for his technical assistance.

References and Notes

(1) Mita, I.; Horie, K. *J. Macromol. Sci., Rev. Macromol. Chem. Phys.* **1987**, *C27*, 91.
(2) Mahabadi, H. K. *Makromol. Chem., Macromol. Symp.* **1987**, *10/11*, 127.
(3) Tulig, T. J.; Tirrell, M. *Macromolecules* **1982**, *15*, 459.
(4) Benson, S. W.; North, A. M. *J. Am. Chem. Soc.* **1962**, *84*, 935.
(5) Schulz, G. V. *Z. Phys. Chem.* **1956**, *8*, 290.
(6) Gardon, J. L. *J. Polym. Sci., Polym. Chem. Ed.* **1968**, *6*, 2853.
(7) Russell, G. T.; Napper, D. H.; Gilbert, R. G. *Macromolecules* **1988**, *21*, 2133.
(8) Cardenas, J. N.; O'Driscoll, K. F. *J. Polym. Sci., Polym. Chem. Ed.* **1976**, *14*, 883.
(9) Soh, S. K.; Sundberg, D. C. *J. Polym. Sci., Polym. Chem. Ed.* **1982**, *20*, 1299, 1315, 1331.
(10) Olaj, D. F.; Zifferer, G.; Gleixner, G. *Macromolecules* **1987**, *20*, 839.
(11) Ballard, M. J.; Napper, D. H.; Gilbert, R. G.; Sangster, D. F. *J. Polym. Sci., Polym. Chem. Ed.* **1986**, *24*, 1027. Ballard, M. J.; Napper, D. H.; Gilbert, R. G. *J. Polym. Sci., Polym. Chem. Ed.* **1984**, *22*, 3225.
(12) Lansdowne, S. W.; Gilbert, R. G.; Napper, D. H.; Sangster, D. F. *J. Chem. Soc., Faraday Trans. 1* **1980**, *76*, 1344.
(13) Gilbert, R. G.; Napper, D. H. *J. Macromol. Sci., Rev. Macromol. Chem. Phys.* **1983**, *C23*, 127.
(14) Hawkett, B. S.; Napper, D. H.; Gilbert, R. G. *J. Chem. Soc., Faraday Trans 1* **1980**, *76*, 1343.
(15) Hui, A. W.; Hamielec, A. E. *J. Appl. Polym. Sci.* **1972**, *16*, 749.
(16) Ferry, J. D. *Viscoelastic Properties of Polymers*, 3rd ed.; Wiley: New York, 1980.
(17) Mills, I. *Quantities, Units and Symbols in Physical Chemistry*; Blackwell: Oxford, 1988.
(18) Maxwell, I. A.; Morrison, B. R.; Napper, D. H.; Gilbert, R. G., submitted for publication in *Macromolecules*.
(19) von Meerwall, E.; Amis, E. J.; Ferry, J. D. *Macromolecules* **1985**, *18*, 260.
(20) Flory, P. J. *Statistical Mechanics of Chain Molecules*; Interscience; New York, 1969.
(21) Wheeler, L. M.; Lodge, T. P.; Hanley, B.; Tirrell, M. *Macromolecules* **1987**, *20*, 1120.

(22) Dionisio, J.; Mahabadi, H. K.; O'Driscoll, K. F.; Abuin, E.; Lissi, E. A. *J. Polym. Sci., Polym. Chem. Ed.* **1979**, *17*, 1891.
(23) Mahabadi, H. K.; O'Driscoll, K. F. *J. Macromol. Sci., Chem.* **1977**, *A11* (5), 967.
(24) Landry, M. R.; Gu, Q.; Yu, H. *Macromolecules* **1988**, *21*, 1158.
(25) Norrish, R. G. W.; Smith, R. R. *Nature* **1942**, *150*, 336.
(26) Trommsdorff, E.; Köhle, H.; Lagally, P. *Makromol. Chem.* **1947**, *1*, 169.
(27) Turner, D. T. *Macromolecules* **1977**, *10*, 221.
(28) Balke, S. T.; Hamielec, A. E. *J. Appl. Polym. Sci.* **1973**, *17*, 905.
(29) de Gennes, P.-G. *Scaling Concepts in Polymer Physics*; Cornell University Press: Ithaca, NY, 1979.
(30) Tirrell, M. *Rubber Chem. Technol.* **1984**, *57*, 523.
(31) Lodge, T. P.; Wheeler, L.; Hanley, B.; Huang, J. W.; Landry, M. R.; Frick, T. S.; Lee, J. A.; Tirrell, M. *Makromol. Chem. Macromol. Symp.* **1987**, *10/11*, 151.

Registry No. Styrene, 100-42-5.